Research on path planning of quadruped robot based on globally mapping localization

1st Yufei Liu
Unmanned center
China North Vehicle Research Institute
Beijing
liuyufei_hit@163.com

2nd Lei Jiang*
Unmanned center
China North Vehicle Research Institute
Beijing
feist201@qq.com

3rd Fengqian Zou
MEMS center
Harbin Institute of Technology
Harbin
flyinthesky2010@163.com

4th Boyang Xing
Unmanned center
China North Vehicle Research Institute
Beijing
golaced@163.com

5th Zhirui Wang
Unmanned center
China North Vehicle Research Institute
Beijing
zhrwangrobot@bjtu.edu.cn

6th Bo Su
Unmanned center
China North Vehicle Research Institute
Beijing
bosu@noveri.com.cn

***Abstract*—Perception and navigation control is core key technology for the legged robot to adapt to complex terrain and achieve autonomous walking. It is the key to distinguish the legged robot from manned equipment and become a ground unmanned system. In this paper, the SLAM globally localization system based on the lidar point cloud is established, and a localization framework based on the combination of topological measurements is proposed to realize the map reconstruction and localization of the wild environment. Path planning based on Dijkstra algorithm is proposed to implement the globally terrain autonomous navigation task of the quadruped robot, and autonomous obstacle avoidance strategy of the local map for quadruped robot based on the artificial potential field theory is applied considering the motion and vibration of legged robot. The experimental results show that the globally path navigation can accurately plan the optimal path and complete the autonomous obstacle avoidance of the local map. The results have demonstrated the effectiveness of the proposed method and realize the globally field autonomous walking of the quadruped robot.**

Keywords—path planning, localization, quadruped robot, Dijkstra algorithm, autonomous walking

I. INTRODUCTION

In order to realize the quadruped robot walking on unknown rugged terrain, the robot cannot walk on the rugged terrain without perception system though the walking state of the robot can be obtained by the body sensors. The path planning of the quadruped robot based on the terrain modeling can realize the autonomous walking of the legged robot.

The puppy robot developed by Boston Dynamics is a classic quadruped robot, which has been studied in environmental modeling and motion planning [1-2]. The researchers used vision sensors to construct the terrain environment, and three-dimensional topographic map based on vision sensors are generated to path planning [3]. The big dog robot developed by Boston Dynamics is equipped with GPS, IMU, laser and binocular camera sensors [4]. Visual measurement, environment map construction and localization are realized, and the robot's appropriate foothold can be judged by perception [5].

The robot's environmental perception and modeling based on vision sensors is mainly studied by Belter [6]. The combination of vision and inertial navigation sensors can realize the estimation of pose and movement. The research includes terrain recognition, terrain perception, landing foot selection and path planning in the simulated environment [7]. Fankhauser [8] proposed motion planning method based on external visual perception for quadruped robot ANYmal. Based on the obtained terrain elevation map, the safe foot point for swing leg has been planned and the posture optimization method can help robot to climb large obstacles and stairs. The control framework incorporates map modeling, state estimation, motion control and motion planning, and the proposed method is verified on the quadruped robot.

SLAM method based on EKF is the earliest method to solve the localization [9], it will slow down the computation effectiveness when the signpost dimension is higher due to the higher computational complexity of the EKF. The early sparse EIF algorithm used the sparse structure to reduce the amount of calculation. The kind of sparseness of the structure will lead to strong inconsistency of results, so scholars have started to explore the sparse structure of the SLAM problem [10]. The authors also propose sparse filter method based on posture and feature-based sparse filter method [11]. In order to improve the accuracy of the filter algorithm, the sliding window filter method has been proposed to improve the accuracy, and this method include the previous pose for a period of time.

While visual mapping demonstrated closed loop and visual registration to known landmarks has not been widely adopted for field environments. Much works have focused on globally-consistent map, the methods are sensitive to environmental conditions or external signals. Many approaches [12] rely on grid map, height map of the terrain, where each in the local map represents the height at the position. Some scholars used feature matching algorithms to find the corresponding transformation between scans to build elevation map, but they did not address the error propagation issues. The uncertainty of the position and orientation is reflected by growing the variance of the height estimation [13].

Navigation planning can be divided into two parts for legged robots: path planning for global map and foot planning for local map. The global path planning is generally expressed as an optimization problem, where the objective function of optimization is the optimization path. The constraints of the optimization problem are the constraints of the velocity and the constraints of the initial and the end points. The scholars solved the problem by transforming the constrained into an unconstrained problem [14]. The scholars transform the path planning problem into a graph method, including geometric methods and sampling methods. In terms of cost function, the artificially designed cost function is adopted [15], but it is

978-1-7281-8025-0/20/$31.00 ©2020 IEEE

difficult for the artificially designed function to cover the potential problem space, and a cost function method based on teaching is proposed.

The main contribution of this paper is to develop a perception and navigation algorithm aimed at achieving autonomous walking, the SLAM globally localization algorithm is presented to realize the map reconstruction and localization. The path planning for the global and local map are proposed to implement the autonomous navigation task. This paper is organized as follows: Section II introduces the terrain modeling based on laser sensor. Globally mapping localization are formulated in Section III. Section IV introduces the path planning for global and local map, including global path navigation based on Dijkstra algorithm and obstacle avoidance for local map. Finally, comprehensive experiments are presented in Section V. The conclusions are given in Section VI.

II. TERRAIN MODELING BASED ON LASER SENSOR

Lidar can obtain the point cloud information in the complex environment, and three-dimensional topographic map can be established according to the analysis and processing of the point cloud information. In order to describe terrain information more accurately, four coordinate systems are established based on terrain modeling, as shown in Figure 1. The coordinates are the earth coordinate system $\boldsymbol{O_W}$, the body coordinate system $\boldsymbol{O_B}$, the sensor coordinate system $\boldsymbol{O_V}$ and the leg coordinate system $\boldsymbol{O_L}$ [16].

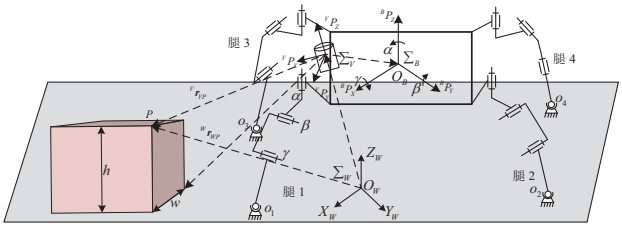

Fig. 1. Coordinate system for terrain modeling framework

Compared with the earth coordinate system, the coordinate of the body coordinate system is ${}^{B}P({}^{B}P_X, {}^{B}P_Y, {}^{B}P_Z)$, the leg coordinate system is ${}^{Li}P({}^{Li}P_X, {}^{Li}P_Y, {}^{Li}P_Z)$, and the sensor coordinate system is ${}^{V}P({}^{V}P_X, {}^{V}P_Y, {}^{V}P_Z)$. In order to establish terrain information based on the center of mass of the body, the lidar information is converted to the body coordinate system:

$$ {}^{B}\boldsymbol{P} = \boldsymbol{T}_{\boldsymbol{B}}^{\boldsymbol{W}} \boldsymbol{T}_{\boldsymbol{V}}^{\boldsymbol{B}} {}^{V}\boldsymbol{P} \tag{1} $$

$\boldsymbol{T}_{\boldsymbol{B}}^{\boldsymbol{W}}$ is conversion matrix between the body coordinate system and the terrain coordinate system, $\boldsymbol{T}_{\boldsymbol{V}}^{\boldsymbol{W}}$ is conversion matrix between the sensor coordinate system and the terrain coordinate system, $\boldsymbol{T}_{\boldsymbol{B}}^{\boldsymbol{W}}$ is obtained from the IMU and the robot sensor data.

The real-time terrain elevation map can be generated according to the obtained point cloud data. The height of each square area in the elevation map can be approximated as a Gaussian probability distribution $\tilde{h} \sim N(h, \sigma_h^2)$, the average height of a single block in the distribution function is h, and the standard deviation is σ_h^2. The position of single object in the sensor coordinate system is defined as ${}^{V}\boldsymbol{r}_{VP}$, the height measurement value in the terrain coordinate system can be obtained by the matrix conversion.

$$ h = \boldsymbol{P}(\mathbf{C}_{VW}^{\mathrm{T}}(\mathbf{q}) {}^{V}\boldsymbol{r}_{VP} - {}^{W}\boldsymbol{r}_{WP}) \tag{2} $$

$\boldsymbol{C}_{VW}^{\mathrm{T}}(\boldsymbol{q})$ is the conversion matrix between sensor and terrain coordinate system, and Unit quaternion array in rotation transformation is $\boldsymbol{q}$.

The standard deviation of the Gaussian probability distribution function is as follows:

$$ \sigma_h^2 = \boldsymbol{J}_V \boldsymbol{\Sigma}_V \boldsymbol{J}_V^{\mathrm{T}} + \boldsymbol{J}_q \boldsymbol{\Sigma}_{h,q} \boldsymbol{J}_q^{\mathrm{T}} \tag{3} $$

The deviation on the measurement of the terrain elevation map has considered the influence of the robot body's posture deviation and the error of sensors. The extended Kalman filter method can be used to fuse the height information of objects to obtain more accurate terrain elevation map. The state variable in data fusion equation is defined as the height information in the terrain elevation map:

$$ \begin{aligned} \boldsymbol{K}_k &= \boldsymbol{P}_k^{-} \boldsymbol{H}_k^{\mathrm{T}} \left(\boldsymbol{H}_k \boldsymbol{P}_k^{-} \boldsymbol{H}_k^{\mathrm{T}} + \boldsymbol{R}_k \right)^{-1} \\ \hat{\boldsymbol{h}}_k &= \hat{\boldsymbol{h}}_k^{-} + \boldsymbol{K}_k \left(\boldsymbol{Z}_k - \boldsymbol{H}_k \hat{\boldsymbol{h}}_k^{-} \right) \\ \boldsymbol{P}_k &= \left(\boldsymbol{I} - \boldsymbol{K}_k \boldsymbol{H}_k \right) \boldsymbol{P}_k^{-} \end{aligned} \tag{4} $$

where $\hat{\boldsymbol{h}}_k$ is the estimated height of obstacle; $\boldsymbol{H}_k$ is identity matrix; $\boldsymbol{P}_k$ is the covariance matrix.

The height measurement value (h, σ_h^2) and the estimated value $(\hat{h}_k, \hat{\sigma}_{hk}^2)$ of the elevation map are fused by the Kalman filter method:

$$ \begin{aligned} \hat{h}_k^{+} &= \frac{\sigma_h^2 \hat{h}_k^{-} + \hat{\sigma}_{hk}^{2-} \tilde{h}}{\sigma_h^2 + \hat{\sigma}_{hk}^{2-}} \\ \hat{\sigma}_{hk}^{2+} &= \frac{\hat{\sigma}_{hk}^{2-} \sigma_h^2}{\hat{\sigma}_{hk}^{2-} + \sigma_h^2} \end{aligned} \tag{5} $$

According to Eq. (2) and Eq. (3), average value and standard deviation of the object height along the robot's forward and horizontal directions can be obtained. The final objective function $(\hat{h}, \hat{\sigma}_h^2)$ can be obtained according to the all point cloud data:

$$ \hat{h} = \frac{\sum_{i=1}^{n} w_i \hat{h}_i}{\sum_{i=1}^{n} w_i}, \hat{\sigma}_h^2 = \frac{\sum_{i=1}^{n} w_i (\hat{\sigma}_i^2 + \hat{h}_i^2)}{\sum_{i=1}^{n} w_i} - \hat{h}^2 \tag{6} $$

where w_i is the current target weight value considering the height information of adjacent grids.

The updated real-time terrain modeling altitude value and altitude standard deviation can be obtained.

III. Globally mapping localization

A. Design for autonomous localization

The autonomous localization module will integrate GPS, IMU and odometer sensor. The navigation module, global map and laser information are fused to complete the accurate posture and location information during autonomous walking of the quadruped robot, which ensure the robot execute accurate global and local path planning.

The autonomous localization of the system needs to consider the global consistency and excessive memory consumption problem of the map cannot be satisfied due to the large disturbance environment. The system adopts dynamic loading of maps method based on the framework of topological measurement localization, and divides global map into a series of local maps and express with scale topological maps. The system adopts the current localization results to dynamically load adjacent maps for information fusion.

B. Window of Optimization based on topological measurement localization

During the localization process, the system adopts window of optimization localization method based on topological measurement. Select a time window based on the current pose, and fuse the GPS, IMU, odometer and point cloud information to form the local localization optimization problem.

The optimized cost function generated by the first content information is defined as C_{odom}. The second and third optimized cost function is defined as C_{loc} and C_Q. The C_{odom} constraint is obtained by mileage interpolation of multi-sensors. The IMU data is obtained according to the integration of the quadruped robot's motion model. The iterative closest point method (ICP) matching with the previous laser data is used to obtain the incremental relative transformation for two adjacent frames. The odometer trajectory is obtained by accumulating a series of relative transformations. It is possible to constrain the relative pose transformation to keep mileage consistent. The posture of the mileage trajectory is defined as U, and the optimization cost function is as follows:

$$C_{odom}=\left\|U_{t-1}^{t}X_{t-1}^{-1}X_{t}\right\|+\left\|U_{t-2}^{t-1}X_{t-2}^{-1}X_{t-1}\right\| \tag{7}$$

Depending on the relative mileage and the previous location, the initial value of the current position relative to the submap can be obtained. The relative pose L_i can be obtained according to the point cloud matching with submap through ICP method. The optimized relative pose can constrain the relative pose transformation between the map and current trajectory. The optimization function can be generated as follows:

$$C_{loc}=\left\|L_{t-2}^{t,-1}M_{i}^{-1}X_{t-2}\right\|+\left\|L_{t}^{j,-1}M_{j}^{-1}X_{t}\right\| \tag{8}$$

The relative pose relationship between maps can be defined as S, and M is the muster for relative pose relationships between all sub maps. The optimization make the sub maps as consistent as possible with the results of map modeling.

$$C_Q=\sum_{i,j\in E}\left\|S_j^{i,-1}M_i^{-1}M_j\right\| \tag{9}$$

The three optimization cost functions can be added to obtain the optimal pose of the current pose relative to the current submap. The final optimization function is as follows:

$$X,M=\min_{X,M}C_{odom}(X)+C_{loc}(X,M)+C_Q(M) \tag{10}$$

After obtaining the optimal X and M, the current localization is transformed by the current moment and sub map.

IV. Path planning for global and local map

A. Global path navigation based on Dijkstra algorithm

The path planning module will complete the global path planning task of the quadruped robot under the global navigation localization map. The Dijkstra algorithm is adopted to plan the navigation path in the global map, and the TEB smoothing algorithm is used to smooth and optimize the global navigation path.

The Dijkstra algorithm is adopted to plan the path in the global grid map, and the initial point is the grid where the robot is currently located. The goal point is the grid where the last target node to be located., The searching space of A* algorithm is much smaller compared with Dijkstra algorithm, and the calculation amount is greatly reduced. However, the generated path is not smooth enough, and it is not the shortest optimal path. The steps of the Dijkstra are as follows:

1) The grid map is defined as G={V,E}, V is the vertex of grid, and E is the side length between the adjacent points. Define S={V_0} at the beginning, T={V-S} are the remaining vertices.

2) Select a vertex W from T that is associated with the vertex of S and has the smallest weight.

3) Modify the distance value of the vertices in the remaining T: if W is added as the middle vertex, the distance value from V_0 to V_1 is shortened, and then modify the distance value.

4) Repeat the second and third steps until S contins the target vertex. After Dijkstra search, the path from the current grid to the target target grid can be obtained.

Due to the low resolution of the grid map, the generated local path needs further processing. The discrete sampling of the grid path can be optimized by the TEB(Timed Elastic Band) algorithm. TEB algorithm adopts g2o to optimize the output of the path points and speeds. The local path nodes are regarded as unknown value, and the constraints between the different nodes are used as conditions. The global path will be smoother and the distance between obstacles can be adjusted.

B. Obstacle avoidance for local map based on potential field theory

The position and height information of the obstacle can be judged by the adjacent grids, and the robot needs to steer when it is detected that the obstacle exceeds the height of the robot or the range of the swing height. The local grid size of the map

is defined as $M \times N$, and the single grid size is $a \times a$, and the grid information format is $g^{[p,q]} = \{x_i^W, y_i^W, z_i^W\}$ as follows:

$$g^{[p,q]} = \begin{Bmatrix} \boldsymbol{P}_i^W \mid (p-1)a \le x_i^W \le pa, \\ (q-1)a \le y_i^W \le qa, i = 1,\ldots k \end{Bmatrix} \tag{11}$$

The height information of obstacles in the grid map can be expressed as $h^{[p,q]}$, which represents the average height for the specific area of terrain.

$$h^{[p,q]} = \frac{\sum_{i=1}^{k} z_i^W}{k} \tag{12}$$

$h^{[p,q]}$ can evaluate the geometric information of the terrain, the height difference between each grid can be defined as:

$$\delta_h^W(i) = z_i^W - z_{i-1}^W \tag{13}$$

In this paper, the body and four legs are approximately equivalent to a virtual body model, and an autonomous obstacle avoidance strategy based on artificial potential field theory is proposed. The method simulates the principle of gravitational field to express the relationship between target position, obstacle position and movement direction of robot. $\boldsymbol{U}_o$ is defined as the repulsive force of obstacles to the robot, and $\boldsymbol{U}_d$ is defined as the attraction force of obstacles to the robot, the system potential can be expressed as:

$$\mathbf{U}_s = \mathbf{U}_o + \mathbf{U}_d \tag{14}$$

According to the model proposed by Khatib [17], the attractive potential function is as follows:

$$\mathbf{U}_d = \frac{1}{2} \cdot k_d \cdot (\mathbf{X}_r^W - \mathbf{X}_d^W)^2 \tag{15}$$

where k_d is the gain coefficient between robot and target position, $\mathbf{X}_r^W$ and $\mathbf{X}_d^W$ are the positions of robot and target respectively.

The potential function generated by repulsive force is as follows:

$$\mathbf{U}_o = \frac{1}{2} \cdot k_o \cdot (\frac{1}{\rho} - \frac{1}{\rho_0})(\mathbf{X}_o^W - \mathbf{X}_d^W)^n \tag{16}$$

where k_o is the gain coefficient between robot and target position, ρ and ρ_0 are the shortest distance and threshold constant of obstacle potential field range respectively.

Combining the potential function generated by attractive and repulsive force, the evaluation function of obstacle avoidance can be obtained as:

$$f(n) = \frac{1}{2} \cdot k_o \cdot (\frac{1}{\rho} - \frac{1}{\rho_0})(\mathbf{X}_o^W - \mathbf{X}_d^W)^n + \frac{1}{2} \cdot k_d \cdot (\mathbf{X}_r^W - \mathbf{X}_d^W)^2 \tag{17}$$

The position of the robot on the map is defined as $G_{n,n}$, and the positions of adjacent grid maps are $G_{n-1,n-1}$ and $G_{n+1,n}$ respectively. According to the distance between the robot and obstacle, the optimal movement direction of the robot to avoid obstacles are calculated, as shown in Fig. 2.

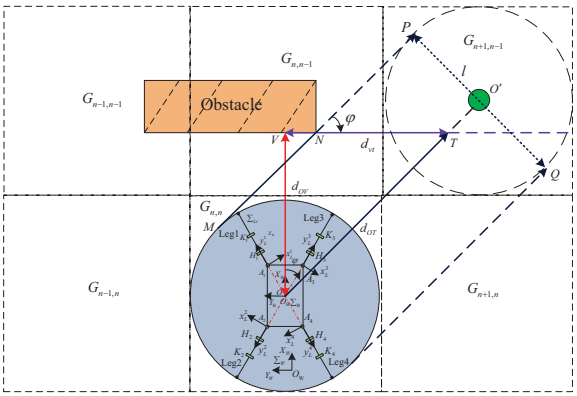

Fig. 2. Optimal locomotion direction for virtual trunk body model

Based on the data obtained from the terrain elevation map, d_{OV} and d_{OT} can be calculated as vertical distance and optimal direction distance. The evaluation function of robot obstacle avoidance based on artificial potential field method is presented, and the yaw angle of obstacle avoidance can be calculated as:

$$\varphi = \arccos\left(\frac{d_{OV}}{d_{OT}}\right) \tag{18}$$

The variables of the quadruped robot including velocity, support height, turning radius and body posture with respect to time are selected as $(v_B(t), h_B(t), r_B(t), \alpha(t), \beta(t), \gamma(t))^{\mathrm{T}}$. The turning radius is calculated as:

$$r_B = S / (2\sin(r_w \pi / 4)) \tag{19}$$

where S is the step size of the body center, and r_w is the steering parameters.

The target position of the trunk body according to the yaw angle during the turning process is generated as:

$$\begin{pmatrix} {}^{B_2}P_{\mathrm{L}}^x \\ {}^{B_2}P_{\mathrm{L}}^y \\ {}^{B_2}P_{\mathrm{L}}^z \\ 1 \end{pmatrix} = {}_{B_1}^{B_2}T^{-1} \begin{pmatrix} {}^{B_1}P_{\mathrm{L}}^x \\ {}^{B_1}P_{\mathrm{L}}^y \\ {}^{B_1}P_{\mathrm{L}}^z \\ 1 \end{pmatrix} = \begin{pmatrix} \left({}^{B_1}P_{\mathrm{L}}^x - S\right)\cos(\frac{r_w\pi}{4}) + Y_0 \sin(\frac{r_w\pi}{4}) \\ \left(S - {}^{B_1}P_{\mathrm{L}}^x\right)\sin(\frac{r_w\pi}{4}) + Y_0 \cos(\frac{r_w\pi}{4}) \\ {}^{B_1}P_{\mathrm{L}}^z \\ 1 \end{pmatrix} \tag{20}$$

The autonomous obstacle avoidance movement in the local map of the quadruped robot is achieved based on potential field theory.

V. Experimental Verification

According to the proposed global and local map navigation localization and path planning method, the perception system is installed on the quadruped robot and the field autonomous experiments have been carried out. The quadruped robot and perception system are shown in Fig. 3.

Fig. 3. The quadruped robot and perception system

Experimental results prove that the quadruped robot meet the above tracking trajectory and velocity requirements. The frequency of the perception planning decision is 5 Hz, and the frequency of emergency obstacle decision and localization update are 10 Hz and 50 Hz. The field experimental performance test of quadruped robot is shown in Fig. 4.

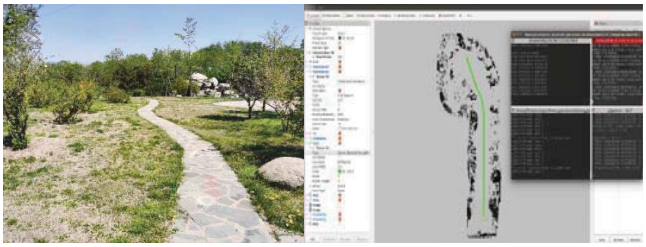

Fig. 4. The field experimental performance test of quadruped robot

The localization method needs to reduce the number of features used to calculate the pose, and the localization adopts point features and robust line features. In order to show the effect of the localization method of the topic, the authors count the successful located positions for different methods on the entire trajectory and the number of corresponding correct feature matches have found. The proposed localization method is compared with P3P method, and results show significantly more successful as shown in Fig. 5. The number of correct feature matches is also greater; thus, the results indicate that the localization method is more robust.

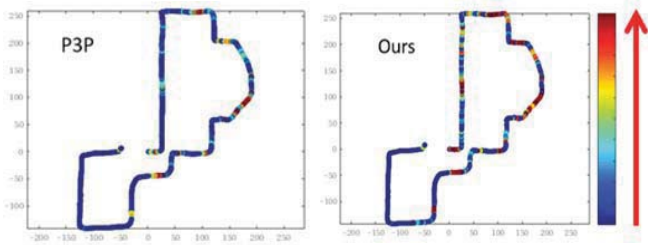

Fig. 5. Number of successful localization

As shown in Fig.4, the path points given by the perception system are 20, and the first point 47.245m is the target point and the closest point tracked by the robot is 0.3m. The subsequent points can be set according to the sparseness of the path points. The optimal green trajectory generated based on Dijkstra algorithm ensures that the robot can walk along the optimal path in the global localization map, and the path diversification of quadruped robot during walking is as shown in Fig. 6. The localization and movement process of the quadruped robot is as shown in Fig. 6 (a)-(d). The robot tracks the global path and reaches the global goal point. The accuracy of the global localization map and the feasibility of the path can be proved as shown in Fig. 6.

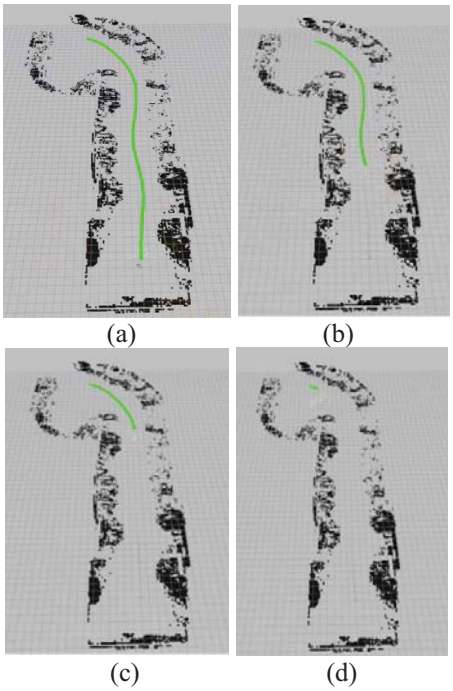

Fig. 6. Path diversification of quadruped robot during walking

In order to verify that the robot can track and avoid obstacles in the local map by the command from laser sensors, the authors compare the yaw angle based on laser with the yaw angle based on kinematics, as shown in Fig. 7.

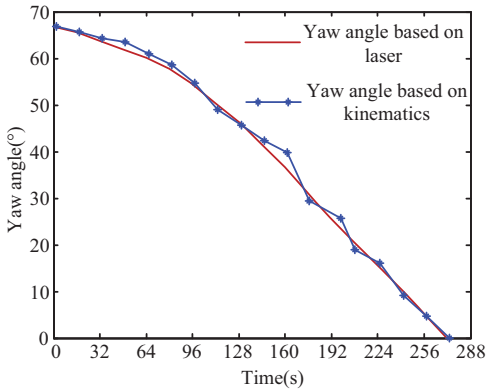

Fig. 7. Optimal locomotion direction for virtual trunk body model

The red solid line in Fig. 7 represents that the optimal feasible steering angle obtained by obstacle avoidance evaluation function. The blue star line represents the yaw angle calculated by the robot movement kinematics. The experimental comparison verifies that the robot can track the yaw angle real time and realize the obstacle avoidance. The feet swing and stance trajectory curves are obtained by the body sensors as shown in Fig. 8

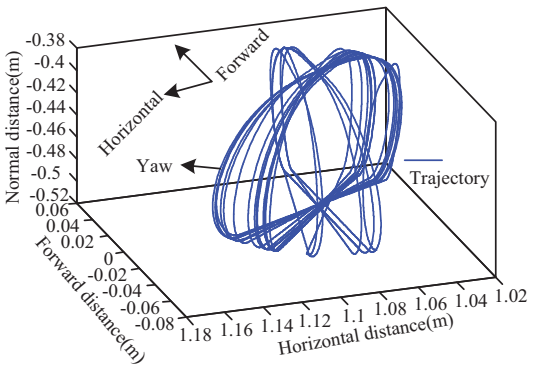

Fig. 8. Swing and stance trajectory curves of single leg

The obstacle avoidance movement process of quadruped robot is shown in Fig. 9. Due to the large envelope of obstacles in the local map, the robot completes the autonomous obstacle avoidance movement according to the local map and obstacles information from the laser sensors real time.

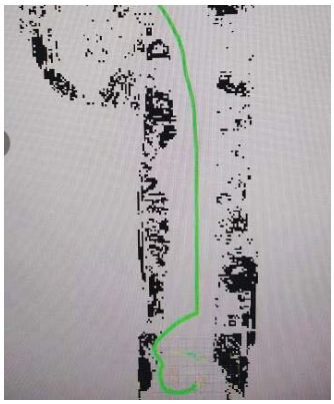

Fig. 9. Optimal locomotion direction for virtual trunk body model

VI. Conclusion

In this study, we investigate a perception and navigation algorithm aimed at achieving autonomous walking. The validity of the algorithm is evaluated by using a quadruped prototype. The conclusions are as follows:
(1) SLAM globally localization algorithm is presented to realize the map reconstruction and localization of the field environment; (2) Path planning based on Dijkstra algorithm is proposed to implement the globally terrain autonomous navigation task of the quadruped robot; (3) Autonomous obstacle avoidance strategy of the local map for quadruped robot based on the artificial potential field theory is applied considering the movement and vibration of legged robot; (4) Comprehensive experiments for the algorithm are carried out, and the results validate the theoretical analysis. Further research will be conducted for the foothold optimization on the field terrains, and high tracking performance for the obstacle avoidance will be considered in the future.

Acknowledgment

This study was supported by the National Key Research and Development Program of China (Grant No. SQ2019YFB130016). Beijing Science and Technology Project (No. Z191100008019009). National Natural Science Foundation of China (Grant No. 91748211). Foundation of Chinese State Key Laboratory of Robotics and Systems (Grant No. SKLRS201501B, SKLRS20164B).

References

[1] J. Kolter, M. Rodgers, A. Ng, “A control architecture for quadruped locomotion over rough terrain,” Proc. of the International Conference on Robotics and Automation, pp. 811–818, 2008.

[2] M. Kalakrishnan, J. Buchli, P. Pastor, “Learning locomotion over rough terrain using terrain templates,” Proc. of the International Conference on Intelligent Robots and Systems, pp. 167-172, 2009.

[3] P. Filitchkin, K. Byl, “Feature-based terrain classification for littledog,” Proc. of the International Conference on Intelligent Robots and Systems, pp. 1387-1392, 2012.

[4] B. Mitchell, A. Hofmann, B. Williams, “Search-based foot placement for quadrupedal traversal of challenging terrain,” Proc. of the International Conference on Robotics and Automation, pp. 1461–1466, 2007.

[5] M. Raibert, K. Blankespoor, G. Nelson, Bigdog, “the rough-terrain quadruped robot,” Proc. of the 17th World Congress, vol. 17, pp. 10822-10825, 2008.

[6] D. Belter, P. Labecki, P. Skrzypczynski, “Map-based adaptive foothold planning for unstructured terrain walking,” Proc. of the International Conference on Robotics and Automation, pp. 5256-5261, 2010.

[7] D. Belter, P. Skrzypczynski, “Rough terrain mapping and classification for foothold selection in a walking robot,” Journal of Field Robotics, vol. 28, pp. 497-528, 2011.

[8] P. Fankhauser, M. Bjelonic, C. Bellicoso, “Robust rough-terrain locomotion with a quadrupedal robot,” Proc. of the International Conference on Robotics and Automation, pp. 5761-5768, 2018.

[9] M. Dissanayake, Gamini, “A solution to the simultaneous localization and map building(SLAM) problem,” IEEE Transactions on Robotics & Automation, 2001.

[10] S. Thrun, “ Simultaneous localization and mapping with sparse extended information filters, ” International Journal of Robotics Research, vol. 23, pp. 693-716, 2004.

[11] R. Matthew, M. Ryan, “Exactly sparse extended information filters for feature-based slam,” The International Journal of Robotics Research, vol. 26, pp. 335-359, 2007.

[12] Mastalli C, Focchi M, “Trajectory and foothold optimization using low-dimensional models for rough terrain locomotion,” in IEEE International Conference on Robotics and Automation (ICRA), pp. 1096-1103, 2017.

[13] Kleiner A, Dornhege C, “Real-time localization and elevation mapping within urban search and rescue scenarios,” Journal of Field Robotics, vol. 24, pp. 723-745, 2007.

[14] P. Fankhauser, M. Bjelonic, C. D. Bellicoso, “Robust rough-terrain locomotion with a quadrupedal robot,” Proc. of the International Conference on Robotics and Automation, pp. 5761-5768, 2018.

[15] D. Kanoulas, A. Stumpf, V.S. Raghavan, “Footstep planning in rough terrain for bipedal robots using curved contact patches,” Proc. of the International Conference on Robotics and Automation, pp. 4662-4669, 2018.

[16] Y. F. Liu, L. Ding, H. B. Gao, “Autonomous obstacle avoidance control of heavy-duty hexapod robot for lunar exploration based on laser ranging,” Journal of Astronautics, vol. 39, pp. 1381-1390, 2018.

[17] O. Khatib, “Real-time obstacle avoidance for manipulators and mobile robots,” International Journal of Robotics Research, vol. 5, pp. 90-98, 1986.